Spectroscopy Letters: An International Journal for Rapid Communication

Publication details, including instructions for authors and subscription information:
http://www.tandfonline.com/loi/lstl20

Influence of Diffusion Parameters on the Spectral Characteristics of Raman Modes of Titanium-Diffused Lithium Niobate Planar Waveguides

José M. M. M. de Almeida [a] [b] & J. Agostinho Moreira [c]

[a] INESC Porto, Rua do Campo Alegre , Porto , Portugal

[b] Departamento de Física da Escola de Ciências e Tecnologia da Universidade de Trás-os-Montes e Alto Douro , Vila Real , Portugal

[c] IFIMUP and IN-Institute of Nanoscience and Nanotechnology , Departamento de Física e Astronomia da Faculdade de Ciências da Universidade do Porto, Rua do Campo Alegre , Porto , Portugal

Accepted author version posted online: 05 Feb 2013.Published online: 22 May 2013.

To cite this article: José M. M. M. de Almeida & J. Agostinho Moreira (2013) Influence of Diffusion Parameters on the Spectral Characteristics of Raman Modes of Titanium-Diffused Lithium Niobate Planar Waveguides, Spectroscopy Letters: An International Journal for Rapid Communication, 46:6, 453-458, DOI: 10.1080/00387010.2012.755704

To link to this article: http://dx.doi.org/10.1080/00387010.2012.755704

Spectroscopy Letters, 46:453–458, 2013

ISSN: 0038-7010 print/1532-2289 online
DOI: 10.1080/00387010.2012.755704

Taylor & Francis
Taylor & Francis Group

Influence of Diffusion Parameters on the Spectral Characteristics of Raman Modes of Titanium-Diffused Lithium Niobate Planar Waveguides

José M. M. M. de Almeida[1,2], and J. Agostinho Moreira[3]

[1]INESC Porto, Rua do Campo Alegre, Porto, Portugal
[2]Departamento de Física da Escola de Ciências e Tecnologia da Universidade de Trás-os-Montes e Alto Douro, Vila Real, Portugal
[3]IFIMUP and IN-Institute of Nanoscience and Nanotechnology, Departamento de Física e Astronomia da Faculdade de Ciências da Universidade do Porto, Rua do Campo Alegre, Porto, Portugal

ABSTRACT A systematic investigation on the influence of the diffusion parameters (time and temperature) and initial titanium film thickness on the spectral characteristics of the $LiNbO_3$ Raman modes is reported. Raman spectra are measured in the range 50–1000 cm^{-1} ~2 μm below the surface of the crystals. Broadening of the Raman lines and, therefore, crystal lattice disorder induced by the titanium ions are found to depend on the fabrication parameters. The disorder associated with the titanium ions near the surface of $LiNbO_3$ is encoded in the broadening of the $A_1(TO_1)$ Raman line. A linear relation between the $A_1(TO_1)$ mode broadening and the Ti concentration is presented. The diffusion theory is used to explain the experimental data. Raman spectroscopy combined with diffusion theory can be used to estimate the evolution of the titanium surface concentration.

KEYWORDS lithium niobate, raman spectroscopy, Ti-diffused waveguides

INTRODUCTION

Lithium niobate ($LiNbO_3$) is one of the most used dielectric materials for integrated optics devices, due to its excellent electro-optic, acousto-optic, and nonlinear properties.[1] A large variety of integrated devices have been demonstrated in $LiNbO_3$, such as phase and amplitude modulators, acoustic filters, spectrum analyzers, and SHGs.[2] Integrated lasers and amplifiers were made possible by doping with rare earths Nd, Yb, and Er or with Cr.[3,4] Ti:$LiNbO_3$ waveguides are fundamental components for production of quasi-phase-matched nonlinear integrated optics devices, which have high conversion efficiency.[5]

High-performance waveguides based on $LiNbO_3$ are obtained by proton-exchange or Ti diffusion.[1] Propagation losses of 0.1 dB cm^{-1} can be attainable if special care is taken in the Ti film deposition process. The commercially available congruent $LiNbO_3$ wafers have high optical quality

Received 13 October 2012; accepted 2 December 2012.

Address correspondence to José M. M. M. de Almeida, Departamento de Física da Escola de Ciências e Tecnologia da Universidade de Trás-os-Montes e Alto Douro, Apartado 1013, 5001-801 Vila Real, Portugal. E-mail: jmmma@utad.pt

and uniformity. However, local heterogeneities in undoped substrates can exist or can be originated by the Ti diffusion process.

The lattice dynamics of pure $LiNbO_3$ have been extensively studied both experimentally and theoretically, and the mode assignment of the observed Raman bands is well established.[6,7] It has been shown that micro-Raman spectroscopy can be used to monitor the quality of the $LiNbO_3$ substrate,[8] Ti-diffused waveguides,[9] Fe-diffused and $LiNbO_3$,[10] and to study the effect of rare earth doping of $LiNbO_3$.[11,12]

The diffusion of Ti on $LiNbO_3$ has been experimentally studied by several authors through different techniques.[1] Very recently, secondary ion mass spectrometry was used to study the diffusion properties of Ti^{4+} ions in an optical damage–resistant Ti:Mg:$LiNbO_3$ waveguide structure.[13] A quantitative relation between the $E(TO_1)$ mode broadening and the Ti concentration was presented in reference [14].

Despite the extensive research carried out, a systematic study of the effect of diffusion parameters on the A_1 vibration modes of Ti-diffused $LiNbO_3$ substrates is still missing.

The aim of this work is to study the influence of the diffusion parameters (time and temperature) and initial Ti film thickness on the broadening of the A_1 Raman active bands induced by Ti. The diffusion theory is used to explain the observed broadening of the Raman lines and, therefore, the crystal lattice disorder induced by the Ti ions. From the experimental and published data, a linear relation between the $A_1(TO_1)$ mode broadening and the Ti concentration was determined.

BRIEF SUMMARY OF DIFFUSION THEORY

The Ti concentration profile due to thermal diffusion from a thin film, before film depletion (thick film regime), is given under conditions of non–steady state by:[15]

$$C(x,T,t) = C_M\, erfc\left(\frac{x}{2\sqrt{Dt}}\right) \tag{1}$$

where C_M is the surface concentration of the substrate, given by the solubility of the ions in the crystal; t and T are the time and the temperature of diffusion, respectively; and D is the diffusion coefficient, which is an exponential function of temperature.[13] When the diffusion time is longer than the film depletion time (thin film regime), the concentration profile can be approximated by a Gaussian function:[16]

$$C(x,T,t) = C_{surf} \exp\left(-\frac{x^2}{d^2}\right) \tag{2}$$

$$C_{surf} = \frac{C_0 h}{\sqrt{\pi D t}} \tag{3}$$

where $C_0 h$ is the quantity of the material deposited on the surface, h is the film thickness, d is the diffusion depth, and C_{surf} is the surface concentration.

EXPERIMENTAL DETAILS

In this work, $LiNbO_3$ samples ($15 \times 8\,mm^2$) were cut from an X-cut 1 mm thick wafer of a congruent crystal. Ti films, with thicknesses of 50, 75, 100, and 200 nm, were deposited by thermal evaporation, using an electron beam (Edwards Auto 306, Edwards, London, UK), on the polished side of the samples. The samples were placed in a tubular furnace and a flux of 1.0 dm^3/min of dry oxygen was set. Diffusion was performed at temperatures from 1030°C to 1130°C, over periods of time from 2 to 48 hr.

The polarized Raman spectra have been recorded, in the 50–1000 cm^{-1} spectral range, at room temperature. The 514.5 nm linear polarized line of an Ar^+ laser was used. The incident laser power impinging on the sample was kept below 100 mW to avoid local heating on the sample. The samples were placed in a confocal Olympus microscope (Olympus, New York, NY, USA), equipped with a $100\times$ objective (NA = 0.95), which was used to focus the laser beam on the sample and for collecting the Raman scattered signal in the backscattering geometry. The orientation of the linear polarization of the laser line can be changed by using a half-wave plate for the 514.5 nm line, and the Raman scattered light was filtered by using a polarized line.

The scattered light was analyzed using a T64000 Jobin-Yvon spectrometer (HORIBA, Longjumeau, France), operating in triple subtractive mode, and equipped with a liquid nitrogen–cooled charge-coupled device. Using 1800 lines/mm holographic gratings and taking into account the 3×640 mm focal length, the spectrometer spectral resolution is

$0.15\,cm^{-1}$. Identical conditions were maintained for all scattering measurements.

The laser spot size was estimated to be ~1 μm in diameter; taking into account the confocal implementation of the microscope, we are probing phonons near 2 μm below the surface of the sample. Identical conditions were maintained for all scattering experiments. The spectral slit width was about $1.5\,cm^{-1}$, which is the spectral resolution of the measurement. The Raman spectra were collected in the x(ZZ)x scattering geometry, which allows us to access to the A_1 phonon modes. The polarized Raman scattered radiation was collected from the surface of a set of Ti:$LiNbO_3$ samples, fabricated at different diffusion conditions.

To get information regarding the frequency and the full-width half-maximum (FWHM) of the relevant Raman bands, a sum of independent damped oscillators was fitted to the experimental spectra:[17]

$$I(\omega, T) = [1 + n(\omega, T)] \sum_{j=1}^{N} A_{oj} \frac{\omega \Omega_{oj}^2 \Gamma_{oj}}{\left(\Omega_{oj}^2 - \omega^2\right)^2 + \omega^2 \Gamma_{oj}^2} \quad (4)$$

Here, $n(\omega, T)$ is the Bose-Einstein factor, and A_{oj}, Ω_{oj}, and Γ_{oj} are the oscillator strength, wavenumber, and damping coefficient of the jth oscillator, respectively. Equation (4) has been widely used by several authors to perform the Raman spectra deconvolution. Although this procedure doesn't take into account mode coupling, it is suitable for determination of the relevant parameters describing each band.[18] The error in the determination of the full-width half-maximum is better than 5%.

RESULTS AND ANALYSIS

Lithium niobate crystal at room temperature belongs to the *R3c* space group and contains two formula units (10 atoms) giving 27 optical degrees of freedom: 18 vibrational modes at the Γ-point are decomposed into $\Gamma = 4A_1 + 5A_2 + 9E$.[6] The A_2 phonons are Raman inactive, while the A_1 and E modes are both Raman and infrared active. To probe the A_1 modes the incident and the scattered light must be polarized along the c-axis (optical axis).

Moreover, to get reliable data for discussion, we have studied the Raman signal coming from the same depth of the cross-section of the samples. This procedure allows us to only study the effect of diffusion parameters on the Raman bands in the same conditions in all samples. The study of the Raman signal coming from different depths is running and the analysis of the experimental data is more complex, and it will give information regarding the diffusion pattern and be published elsewhere.

Figure 1 shows the x(ZZ)x Raman spectra (A_1(TO) modes) of the undoped congruent $LiNbO_3$ and of Ti-diffused $LiNbO_3$ samples, coated with 100 nm Ti thin film and diffused at 1080°C for 2, 28, and 40 hr, respectively. The Raman spectrum of pure $LiNbO_3$ agrees with the results presented in current literature.[5] No new Raman bands could be detected on the Ti-diffused samples.

The frequency of the Raman bands remains unaffected within the experimental error, in accordance with previous results.[9,19] This result can be understood taking into account the specific vibrational modes observed in the 100–900 cm^{-1} spectral range. The $A_1(TO_4)$ mode is assigned to the in-phase stretching Nb-O modes, involving movement of the oxygen atoms of the NbO_6 octahedra, while the B-site atom remains stationary. The remaining A_1(TO) modes involve the out-of-phase vibration of the oxygen plan against the Nb ions, while the A-site

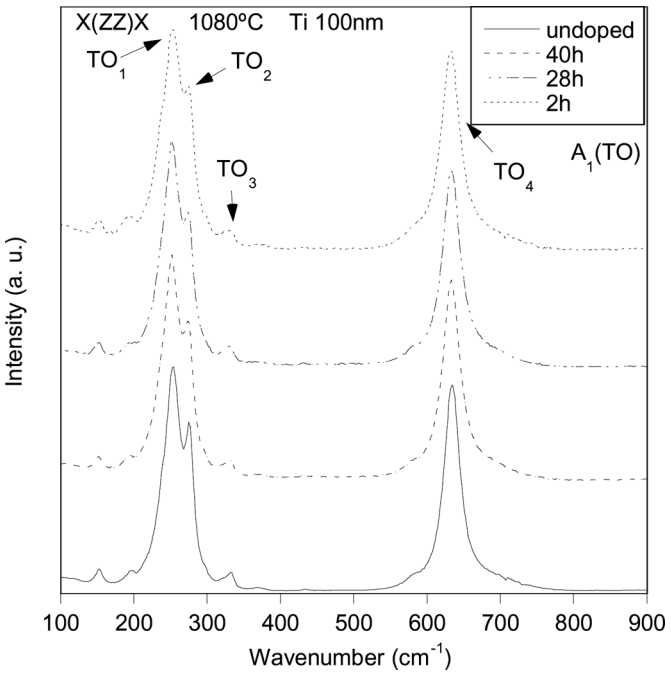

FIGURE 1 Raman spectra (A_1(TO) modes) of undoped congruent $LiNbO_3$ and Ti-diffused $LiNbO_3$ at 1080°C for 2, 28, and 40 hr. The initial Ti film thickness was 100 nm.

ions remain stationary. These modes involve the changes on the Nb-O bond lengths and their frequency is known to be strongly dependent on the covalent bond Nb-O strength and, thus, little affected by the substitution of the Li ions by Ti ones. The absence of frequency shifts in this kind of mode was already reported in Y- or Lu-doped $EuMnO_3$.[18]

This issue evidences that diffused Ti atoms do not alter the crystal structure of the $LiNbO_3$ matrix. So, the effect of the introduction of Ti in the system is to enhance disorder, which can be studied through the dependence of the FWHM of the Raman bands on the diffusion parameters. For this purpose, Eq. (1) was fitted to the experimental spectra presented in Fig. 1. We have chosen to study the FWHM of two particular modes: the $A_1(TO_1)$ lattice mode and the internal $A_1(TO_4)$ mode. Both modes are found to be sensitive to the crystal disorder. The FWHM of the corresponding bands reflects the disorder in the Nb sublattice induced by the Ti diffusion process.

Figure 2 depicts the FWHM of the $A_1(TO_1)$ band as a function of $t^{-1/2}$, after diffusion of a 100 nm thick Ti film at 1030°C, 1080°C, and 1130°C. For a constant diffusion temperature, the FWHM decreases with increasing diffusion time, and for constant diffusion time, a higher temperature leads to a lower FWHM. The solid lines in Fig. 2 were calculated from the best fit of the linear function on $t^{-1/2}$ to the FWHM data. The horizontal dashed line represents the FWHM of the $A_1(TO_1)$ band for virgin $LiNbO_3$ crystal. The extrapolation of the linear relations (dashed lines on the left side of Fig. 2) converges as the diffusion time increases. In the limit $t \to \infty$, the FWHM values tend to the undoped $LiNbO_3$ value. This result clearly shows that for very large values of the diffusion time the FWHM of undoped crystals should be attained.

The aforementioned $t^{-1/2}$ dependence of the TO_1 FWHM mode can be understood in the following way. According to diffusion theory,[13] the Ti surface concentration decreases as the diffusion time increases, the rate of decrease being larger for higher temperatures.

A high value of the FWHM, compared with the corresponding value of the virgin $LiNbO_3$, indicates that initially a high lattice disorder exists, which agrees with the fact that surface concentration is larger when the diffusion process starts. As time increases, the Ti ions diffuse deeper in the crystal, and the surface concentration must decrease. For higher diffusion times, lower value of the FWHM points to a partially restored crystalline order on the surface of the samples.

Figure 3 depicts the FWHM of the $A_1(TO_1)$ band as a function of the Ti surface concentration after

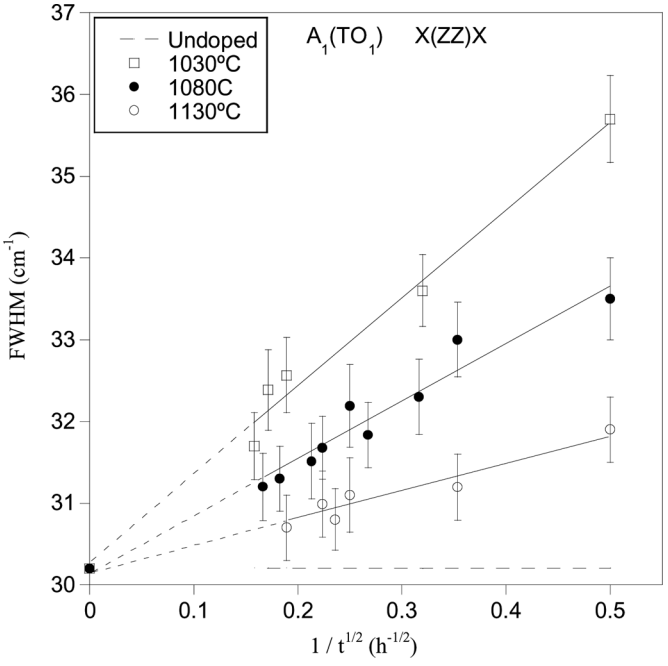

FIGURE 2 **FWHM of the $A_1(TO_1)$ mode for samples diffused at 1030°C, 1080°C, and 1130°C, as a function of time. The horizontal dashed lines represent the FWHM of the $A_1(TO_1)$ band for virgin $LiNbO_3$ crystal.**

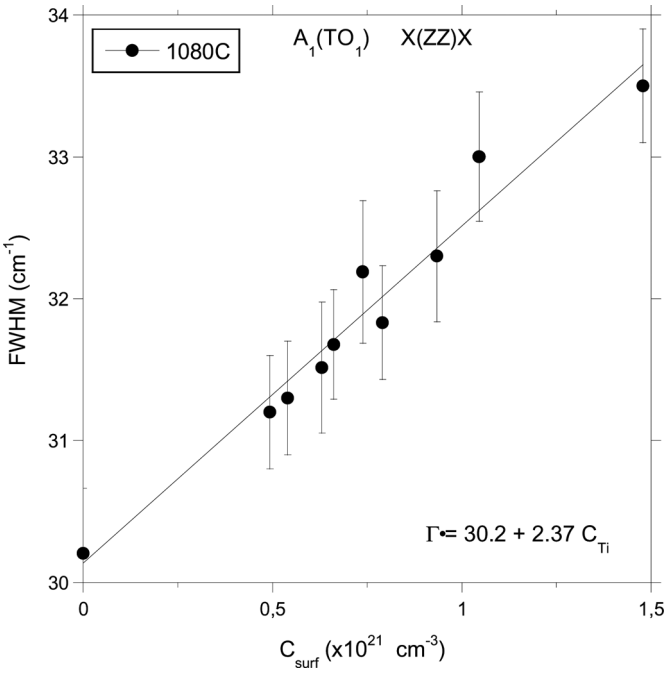

FIGURE 3 **FWHM of the $A_1(TO_1)$ mode as a function of the Ti surface concentration after diffusion of a 100 nm thick Ti film at 1080°C.**

diffusion of a 100 nm thick Ti film at 1080°C. The values of the Ti surface concentration were calculated from the diffusion theory (Eq. 3) using the diffusion constant and activation energy values determined from SIMS measurements.[17]

One can see that the Ti-induced broadening of the $A_1(TO_1)$ mode displays an almost linear relationship to the Ti concentration. The fitted linear relation is given by:

$$\Gamma = 30.2 + 2.37C_{Ti} \quad (5)$$

The diffusion time dependence of the FWHM of the $A_1(TO_4)$ mode was studied. As time increases, the FWHM decreases, but not in the expected $t^{-1/2}$ dependence, as observed for the $A_1(TO_1)$ band. It is worth stressing that the $A_1(TO_4)$ mode is an internal mode, while the $A_1(TO_1)$ is a lattice one. So, the effect of the disorder, arising from the random distribution of Ti on the FWHM, is expected to follow the diffusion Eq. (1) for the lattice mode, but not necessarily for the internal mode, which should be more sensitive to the Nb-O covalent bond than to lattice defects. However, the observed decrease of the $A_1(TO_4)$ band FWHM with diffusion time gives further evidence for the decrease of disorder on the lattice as diffusion time increases. The observed steady decrease corroborates the conclusions drawn above.

Figure 4 shows the FWHM of both the $A_1(TO_1)$ and $A_1(TO_4)$ bands as a function of the initial Ti film thickness, for samples with initial 50, 75, 100, and 200 nm Ti film thickness, diffused at 1080°C for 20 hr. The solid lines in Fig. 4 were calculated from the best fit of the linear relation on initial Ti film thickness to the FWHM data. The Ti diffusion process for this parameter occurs in the finite source regime.[14] A linear increase of C_{surf} with the Ti thickness is expected. For constant diffusion time and temperature, theory predicts an increase of the Ti surface concentration as the Ti film thickness increases, which is in good agreement with the increase of the FWHM of both studied modes.

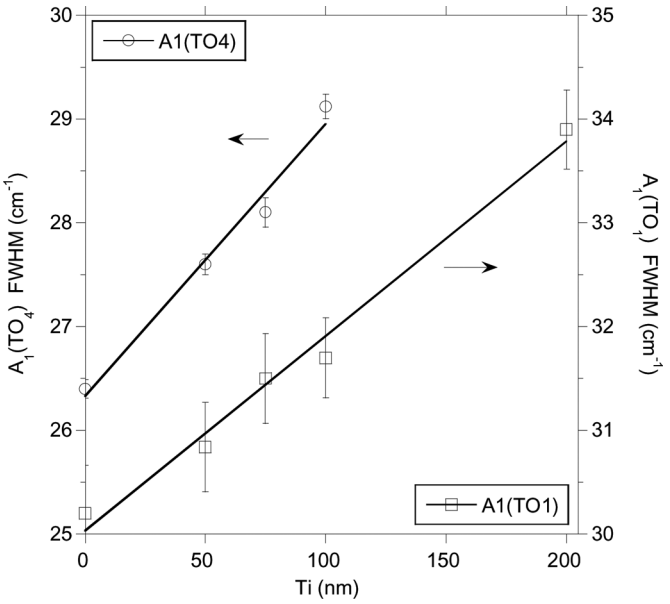

FIGURE 4 FWHM of the $A_1(TO_1)$ and $A_1(TO_4)$ for samples with 50, 75, 100, and 200 nm thick Ti film, diffused at 1080°C during 20 hr.

A set of samples diffused for 2 hr was also considered, and it was shown that the FWHM does not display the same linear variation. For this value of the diffusion time the process occurs in the infinite source regime, the surface concentration being clamped to the maximum value given by the solubility of the Ti ions in $LiNbO_3$. Therefore, Eq. 3 cannot be applied.

Integrated optical devices demand monomode operation. The usual parameters to process such waveguide at ~1 μm are 95 nm Ti film, followed by annealing at 1005°C for 9 hr.[20] Taking into account the results presented here, the crystalline region surrounding the Ti waveguides would retain high disorder.

The absence of new Raman bands on Ti-doped $LiNbO_3$ and significant shifts of the Raman bands give strong evidence that the Ti does not substitute Nb ions. The disorder due to the Ti diffusion process should be associated with either the diffusion of the Ti ions or the Li out-diffusion from the surface of the sample during the annealing process. The studied samples do not reveal any planar optical waveguide in substrates without Ti that stayed in the furnace over long periods of time. To verify if the thermal annealing induces lattice disorder related to Li out-diffusion, a set of samples was annealed at 1130°C for 24, 48, and 72 hr. The obtained value for the FWHM of the $A_1(TO_1)$, $A_1(TO_4)$, $E(TO_1)$, $E(TO_6)$, and $E(TO_8)$ modes was similar, within the experimental error, to the corresponding value for an unannealed sample. It can be concluded that lattice disorder on the surface of the samples cannot be related to Li out-diffusion. Therefore, the general broadening observed in the Raman modes must be due to Ti random distribution in the $LiNbO_3$ lattice.

It is worth stressing that the effect of Ti diffusion is not detected on the frequency of the A_1 and E Raman

active modes. In Raman scattering, the physical property to be probed is the lattice polarizability; so, we can conclude that the lattice polarizability associated with these modes does not change with Ti diffusion. The eletro-optic coefficients are sensitive to the Ti diffusion, but these coefficients are dependent on the electronic polarizability, which is not probed by Raman spectroscopy.

CONCLUSIONS

In summary, we have presented a detailed study of the Raman spectra of Ti-doped $LiNbO_3$ substrates, as a function of diffusion time, temperature, and the initial Ti film thickness. The results obtained give evidence for a random distribution of Ti in the $LiNbO_3$ lattice. Broadening of the Raman lines and, therefore, an increase of the crystal lattice disorder induced by Ti ions were observed. For samples fabricated in the finite source regime, the diffusion theory allowed us to enlighten the experimental results. Complete restoration of the lattice structure in the waveguide region would be attained for high diffusion times, unsuitable for the formation of optical waveguides, which requires high surface concentration of Ti.

From the experimental results a quantitative relation was extracted that allows the use of the FWHM of the $A_1(TO_1)$ Raman mode to calculate the Ti surface concentration on $LiNbO_3$.

REFERENCES

1. Wong, K. K. *Properties of Lithium Niobate*. IEE: London, 2002; 417 pp.
2. Sun, J. A.; Gan, Y.; Xu, C. Q. Efficient green-light generation by proton-exchanged periodically poled MgO:$LiNbO_3$ ridge waveguide. *Opt. Lett.* **2011**, *36*(4), 549–551.
3. Jaque, D. D.; Garcia, J. A. S.; Sole, J. G. Continuous-wave laser oscillation at 929 nm from a Nd3+-doped $LiNbO_3$:ZnO nonlinear laser crystal: a powerful tool for blue laser light generation. *Appl. Phys. Lett.* **2004**, *85*(1), 19–21.
4. Almeida, J. M.; Boyle, G.; Leite, A. P.; Delarue, R. M.; Ironside, C. N.; Caccavale, F.; Chakraborty, P.; Mansour, I. Chromium diffusion in lithium niobate for active optical waveguides. *J. Appl. Phys.* **1995**, *78*(4), 2193–2197.
5. Hu, H.; Nouroozi, R.; Ludwig, R.; Schmidt-Langhorst, C.; Suche, H.; Sohler, W.; Schubert, C. Polarization-insensitive 320-Gb/s in-line all-optical wavelength conversion in a 320-km transmission span. *IEEE Photon. Technol. Lett.* **2011**, *23*(10), 627–629.
6. Ridah, A.; Bourson, P.; Fontana, M. D.; Malovichko, G. The composition dependence of the Raman spectrum and new assignment of the phonons in $LiNbO_3$. *J. Phys. Condens. Matter* **1997**, *9*(44), 9687–9693.
7. Caciuc, V.; Postnikov, A. V.; Borstel, G. Ab initio structure and zone-center phonons in $LiNbO_3$. *Phys. Rev. B* **2000**, *61*(13), 8806–8813.
8. Malovichko, G. I.; Grachev, V. G.; Kokanyan, E. P.; Schirmer, O. F.; Betzler, K.; Gather, B.; Jermann, F.; Klauer, S.; Schlarb, U.; Wohlecke, M. Characterization of stoichiometric $LiNbO_3$ grown from melts containing K_2O. *Appl. Phys. A Mater. Sci. Process.* **1993**, *56*(2), 103–108.
9. Zhang, Y.; Guilbert, L.; Bourson, P. Characterization of Ti:$LiNbO_3$ waveguides by micro-Raman and luminescence spectroscopy. *Appl. Phys. B Lasers Optics* **2004**, *78*(3–4), 355–361.
10. Mignoni, S.; Fontana, M. D.; Bazzan, M. D.; Ciampolillo, M. V.; Zaltron, A. M.; Argiolas, N.; Sada, C. Micro-Raman analysis of Fe-diffused lithium niobate waveguides. *Appl. Phys. B* **2010**, *101*(3), 541–546.
11. Quispe-Siccha, R.; Mejia-Uriarte, E. V.; Villagran-Muniz, M.; Jaque, D.; Sole, J. G.; Jaque, F.; Sato-Berru, R. Y.; Camarillo, E.; Hernandez, J.; Murrieta, H. The effect of Nd and Mg doping on the micro-Raman spectra of $LiNbO_3$ single-crystals. *J. Phys. Condens. Matter* **2009**, *21*(14), 145401.
12. Palatnikov, M. N.; Biryukova, I. V.; Sidorov, N. V.; Denisov, A. V.; Kalinnikov, V. T.; Smith, P. G. R.; Shur, V. Y. Growth and concentration dependencies of rare-earth doped lithium mobate single crystals. *J. Crystal Growth* **2006**, *291*(2), 390–397.
13. Zhang, D. L.; Han, F.; Xu, S. Y.; Hua, P. R.; Pun, E. Y. B. Diffusion properties of Mg^{2+} and Ti^{4+} ions in optical-damage-resistant near-stoichiometric Ti:Mg:$LiNbO_3$ waveguide. *J. Alloys Compounds* **2012**, *541*(15), 269–274.
14. Zhang, D. L.; Zhang, P.; Zhou, H. J.; Pun, E. Y. B. Characterization of near-stoichiometric Ti:$LiNbO_3$ strip waveguides with varied substrate refractive index in the guiding layer. *J. Opt. Soc. Am. A* **2008**, *25*(10), 2558–2570.
15. Crank, J. *The Mathematics of Diffusion*. Oxford University Press: Oxford, U.K., 1975; 414 pp.
16. Caccavale, F.; Chakraborty, P.; Quaranta, A.; Mansour, I.; Gianello, G.; Bosso, S.; Corsini, R.; Mussi, G. Secondary-ion-mass spectrometry and near-field studies of Ti:$LiNbO_3$ optical wave-guides. *J. Appl. Phys.* **1995**, *78*(9), 5345–5350.
17. Moreira, J. A.; Almeida, A.; Ferreira, W.; Araújo, J.; Pereira, A.; Chaves, M. R.; Kreisel, J.; Vilela, S. M.; Tavares, P. B. Coupling between phonons and magnetic excitations in orthorhombic $Eu_{1-x}Y_xMnO_3$. *Phys. Rev. B* **2010**, *81*(5), 054447.
18. Hayes, W.; Loudon, R. *Scattering of Light by Crystals*. John Wiley & Sons: New York, 1978; 211 p.
19. Zhang, D. L.; Siu, G. G.; Pun, E. Y. B. Microscope Raman scattering and X-ray diffraction study of near-stoichiometric Ti:$LiNbO_3$ waveguides. *Phys. Stat. Sol. (a)* **2005**, *202*(13), 2521–2530.
20. Brown, C. T. A.; Amin, J.; Shepherd, D. P.; Tropper, A. C.; Hempstead, M.; Almeida, J. M. 900-nm Nd:Ti:$LiNbO_3$ waveguide laser. *Opt. Lett.* **1997**, *22*(23), 1778–1780.